Supplement of Biogeosciences, 22, 2383–2402, 2025
https://doi.org/10.5194/bg-22-2383-2025-supplement

Biogeosciences Open Access

Supplement of

Effects of submarine groundwater on nutrient concentration and primary production in a deep bay of the Japan Sea

Menghong Dong et al.

Correspondence to: Xinyu Guo (guo.xinyu.mz@ehime-u.ac.jp)

Contents of this file

Text S1 to S4
Tables S1 to S3
Figures S1 to S15

Introduction

This supporting information contains additional descriptions of the model configuration and results (Text S1 to S4), 3 tables (S1−S3) and 15 figures (S1−S15).

Text S1.

A three-dimensional, free surface, primitive equation ocean model was used. It includes thermodynamics and the level 2.5 Mellor-Yamada turbulence closure and uses a sigma coordinate in the vertical to resolve the variation of bottom topography (Blumberg & Mellor, 1987; Mellor, 1998). This model assumes the hydrostatic balance and can be used to solve the nonlinear primitive external and internal mode equations on the Arakawa C-grid system.

Text S2.

Onitsuka and Yanagi (2005) applied two ecosystem models differing in ecological complexity: the NPZD and a nine-compartment model that includes two categories of phytoplankton and three categories of zooplankton, to the northern and southern parts of the Japan Sea with the same biochemical parameters and compared the results of the two models. Their results indicated that the seasonal variations in several variables (such as Chlorophyll-a, nitrate, and primary production) are not significantly different between the two models, and with a careful selection of biochemical parameter values, the NPZD model could calculate the seasonal variations of those variables in the Japan Sea.

Text S3.

The biogeochemical processes in this study are based on nitrogen (Figure S2). The processes related to phosphate were calculated based on a Redfield ratio of 16:1 (N: P). The biogeochemical processes are described as follows:

$$Bio(DIN) = Respiration + Excretion + Decomposition - Photosynthesis, \tag{S1}$$

$$Bio(PHY) = Photosynthesis - Respiration - Mortality(PHY) - Grazing - Sinking, \tag{S2}$$

$$Bio(ZOO) = Grazing - Mortality(ZOO) - Egestion - Excretion, \tag{S3}$$

$$Bio(DET) = Mortality(PHY) + Mortality(ZOO) + Egestion - Decompositon - Sinking, \quad (S4)$$

$$Bio(DIP) = (Respiration + Excretion + Decomposition - Photosynthesis)/16, \quad (S5)$$

Each term of the compartment can be expressed in the forms given below. Photosynthesis is doubled as the water temperature increases by 10 ℃ (Eppley, 1972). An almost identical assumption was adopted for other processes that depend on temperature. The parameter values are shown in Table S1.

$$Photosynthesis = V_{max} \times \min\left\{\frac{DIN}{DIN + K_{DIN}}, \frac{DIP}{DIP + K_{DIP}}\right\} \times \exp(k_{pho}T) \times \frac{I}{I_{opt}} \exp(1 - \frac{I}{I_{opt}}) \times PHY, \quad (S6)$$

$$I = I_0 \exp(-\int_0^z k_e dz), \quad (S7)$$

$$k_e = \alpha_1 + \alpha_2 \times PHY, \quad (S8)$$

$$Respiration = P_{res} \times \exp(k_{res}T) \times PHY, \quad (S9)$$

$$Mortality(PHY) = P_{mor} \times exp(k_{mor1}T) \times PHY^2, \quad (S10)$$

$$Grazing = G_{max} \times \max\{0, 1 - \exp[\lambda(\sigma - PHY)]\} \times exp(k_{gra}T) \times ZOO, \quad (S11)$$

$$Excretion = (\alpha_Z - \beta_Z) \times Grazing, \quad (S12)$$

$$Egestion = (1 - \alpha_Z) \times Grazing, \quad (S13)$$

$$Mortality(ZOO) = Z_{mor} \times exp(k_{mor2}T) \times ZOO^2, \quad (S14)$$

$$Decomposition = D_{dec} \times \exp(k_{dec}T) \times DET, \quad (S15)$$

$$Sinking_{PHY} = \frac{\partial}{\partial z}(S_{PHY} \times PHY), \quad (S16)$$

$$Sinking_{DET} = \frac{\partial}{\partial z}(S_{DET} \times DET), \quad (S17)$$

where I is the light intensity, k_e is the dissipation coefficient, I_0 is the photosynthetically active radiation at the surface, which is considered to be 40% of the shortwave radiation at the surface, and T is the water temperature. A portion (40%) of the surface shortwave radiation data from the GPV-MSM, namely the photosynthetically active radiation, was used as the surface light intensity in photosynthesis (Sarmiento & Gruber, 2006).

Text S4.

Each biogeochemical process supported by different source nutrients in the tracking module can be expressed as follows:

$$Bio_X(DIN) = Respiration \times \frac{PHY_X}{PHY} + Excretion \times \frac{ZOO_X}{ZOO} + Decomposition \times \frac{DET_X}{DET} - Photosynthesis \times \frac{DIN_X}{DIN}, \tag{S18}$$

$$Bio_X(PHY) = Photosynthesis \times \frac{DIN_X}{DIN} - Respiration \times \frac{PHY_X}{PHY} - Mortality(PHY) \times \frac{PHY_X}{PHY} - Grazing \times \frac{PHY_X}{PHY} - Sinking, \tag{S19}$$

$$Bio_X(ZOO) = Grazing \times \frac{PHY_X}{PHY} - Mortality(ZOO) \times \frac{ZOO_X}{ZOO} - Egestion \times \frac{ZOO_X}{ZOO} - Excretion \times \frac{ZOO_X}{ZOO}, \tag{S20}$$

$$Bio_X(DET) = Mortality(PHY) \times \frac{PHY_X}{PHY} + Mortality(ZOO) \times \frac{ZOO_X}{ZOO} + Egestion \times \frac{ZOO_X}{ZOO} - Decompositon \times \frac{DET_X}{DET} - Sinking, \tag{S21}$$

where X can be any of three external sources of nutrient or residual nutrient, i.e., JS, RV, GW, and RE.

Table S1. Average discharge, dissolved inorganic nitrogen (DIN) loading, and dissolved inorganic phosphorus (DIP) loading information for all rivers included in the model.

	River name	Discharge ($m^3 s^{-1}$)	DIN loading ($g s^{-1}$)	DIP loading ($g s^{-1}$)
First-class rivers	Oyabe	32.22	30.62	1.19
	Sho	57.27	14.49	1.48
	Jinzu	92.52	44.43	3.37
	Jyoganji	18.44	5.09	0.5
	Kurobe	38.05	8.46	0.93
Second-class revers	Aogawa	1.47	0.46	0.05
	Shiraiwagawa	4.34	4.47	0.15
	Hojozukata	0.36	1.1	0.09
	Busshojigawa	1.49	3.7	0.09
	Takahashigawa	2.04	2.58	0.07
	Furukawa	0.58	0.33	0.02
	Kurosegawa	1.87	0.83	0.05
	Yoshidagawa	1.18	0.45	0.03
	Sumikawa	3.1	0.94	0.08
	Sakaigawa	2.85	0.42	0.06
	Kiryugawa	0.85	0.3	0.02
	Uchikawa	1.88	1.13	0.08
	Katakaigawa	5.05	1.3	0.11
	Izumigawa	0.98	0.72	0.04
	Irigawa	2.28	0.74	0.05
	Kamichigawa	4.44	1.39	0.11
	Kamikoshogawa	2.66	1.03	0.09
	Sasagawa	1.47	0.25	0.03
	Teragawa	0.4	0.15	0.01
	Shimodagawa	0.71	0.19	0.02
	Shimojogawa	2.4	2.24	0.11
	Ogawa	3.44	0.64	0.07
	Shinborigawa	3.13	2.53	0.13
	Kamogawa	0.64	0.39	0.02
	Yokawagawa	1.59	0.57	0.05
	Unabigawa	0.99	0.29	0.03
	Hayatsukigawa	4.07	0.85	0.09
	Nakagawa	0.68	0.35	0.03

Table S2. Parameters used in the Ecosystem model.

Symbol	Definition	Value	Unit
V_{max}	Maximum photosynthetic rate of PHY at 0 ℃	1.5	d^{-1}
K_{DIN}	Half saturation constant of PHY for DIN	4.5	mmolN m^{-3}
K_{DIP}	Half saturation constant of PHY for DIP	0.12	mmolN m^{-3}
I_{opt}	Optimum light intensity	95	W m^{-2}
k_{pho}	Temperature coefficient for the photosynthetic rate	0.0693	$℃^{-1}$
α_1	Light dissipation coefficient of seawater	0.015	m^{-1}
α_2	Self-shading coefficient of PHY	0.054	$m^2\ mmolN^{-1}$
P_{res}	Respiration rate of PHY at 0 ℃	0.03	d^{-1}
k_{res}	Temperature coefficient for respiration	0.0519	$℃^{-1}$
P_{mor}	Mortality rate of PHY at 0 ℃	0.2	$m^3\ mmolN^{-1}\ d^{-1}$
k_{mor1}	Temperature coefficient for PHY mortality	0.0693	$℃^{-1}$
G_{max}	Maximum grazing rate of ZOO at 0 ℃	0.3	d^{-1}
λ	Ivlev constant of ZOO	1.4	$m^3\ mmolN^{-1}$
σ	The threshold value for grazing PHY	0.043	mmolN m^{-3}
k_{gra}	Temperature coefficient for grazing	0.0693	$℃^{-1}$
Z_{mor}	Mortality rate of ZOO at 0 ℃	0.07	$m^3\ mmolN^{-1}\ d^{-1}$
k_{mor2}	Temperature coefficient for ZOO mortality	0.0693	$℃^{-1}$
α_Z	Assimilation efficiency of ZOO	0.7	Non-dimensional
β_Z	Growth efficiency of ZOO	0.3	Non-dimensional
D_{dec}	Decomposition rate of DET at 0 ℃	0.15	d^{-1}
k_{dec}	Temperature coefficient for decomposition	0.0693	$℃^{-1}$
S_{PHY}	Sinking velocity of PHY	0.1	m d^{-1}
S_{DET}	Sinking velocity of DET	5	m d^{-1}
C/chl.a	The ratio of carbon to Chlorophyll-a	50	Non-dimensional
C/N	Redfield ratio	106/16	Non-dimensional

Table S3. Model validation. rmsd: root mean square deviation; r^2: the coefficient of determination.

	Temperature		Salinity		DIN		Phytoplankton	
	rmsd (°C)	r^2	rmsd (psu)	r^2	rmsd (mmolN m^{-3})	r^2	rmsd (mmolN m^{-3})	r^2
Jan	1.04	0.92	0.15	0.76	2.01	0.90	0.07	0.61
Feb	1.26	0.81	0.12	0.50	2.14	0.93	0.08	0.59
Mar	1.14	0.78	0.16	0.63	0.05	0.96	—	—
Apr	0.90	0.86	0.16	0.85	1.82	0.96	0.06	0.91
May	1.22	0.86	0.27	0.53	1.79	0.95	0.09	0.73
Jun	1.40	0.89	0.23	0.67	1.78	0.96	0.08	0.78
Jul	1.73	0.92	0.25	0.63	2.76	0.90	0.09	0.58
Aug	1.71	0.95	0.26	0.68	2.20	0.93	0.11	0.62
Sep	1.75	0.95	0.30	0.71	—	—	0.06	0.83
Oct	1.34	0.96	0.28	0.75	1.65	0.96	0.09	0.59
Nov	1.16	0.96	0.22	0.75	1.30	0.98	0.06	0.79
Dec	1.06	0.95	0.20	0.66	1.42	0.97	0.02	0.94
Mean	1.75	0.92	0.26	0.64	2.25	0.93	0.08	0.65

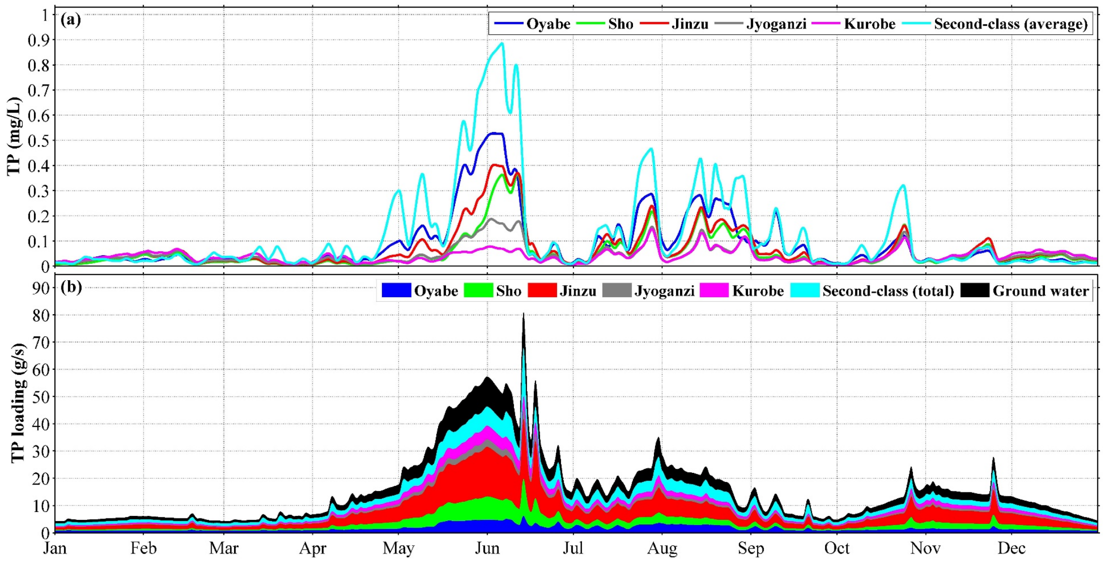

Figure S1. (a) Total phosphate (TP) concentration in the rivers, (b) TP loading from rivers. Dissolved inorganic phosphate (DIP) concentration was specified to be 70% of TP concentration.

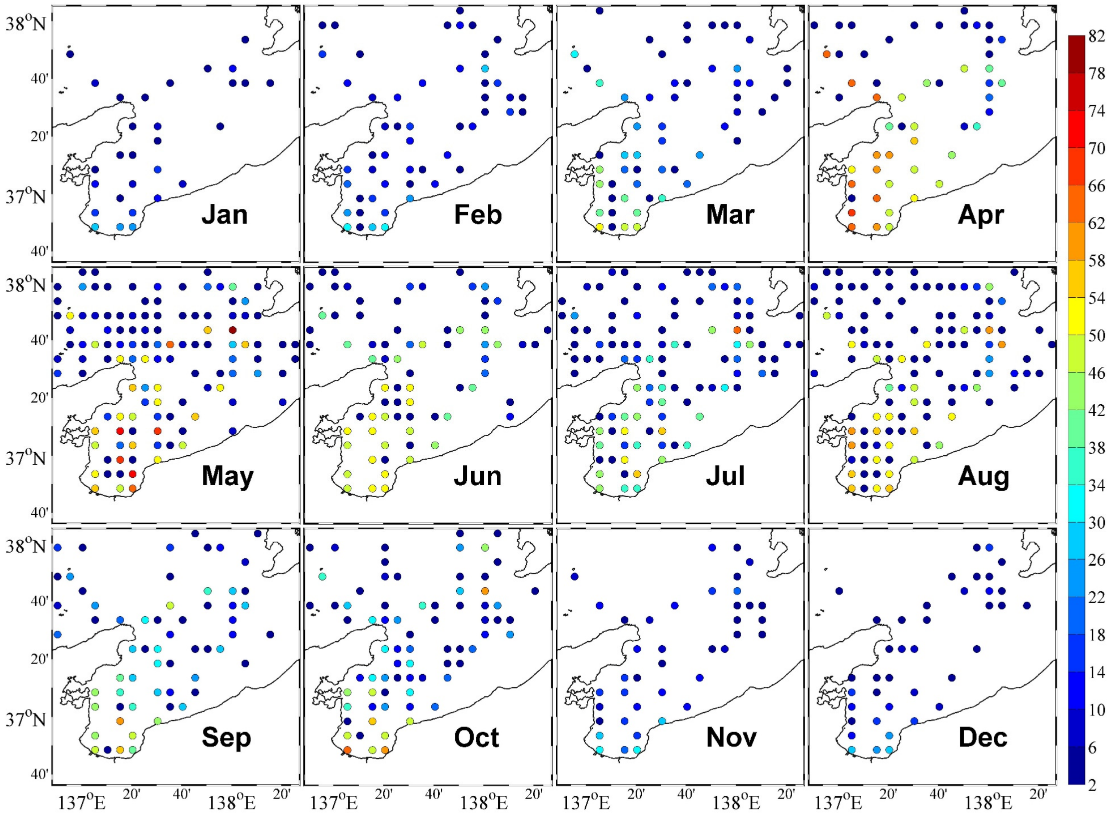

Figure S2. The quantity of observational data available for each grid point from the Marine Information Research Centre (MIRC) Ocean Dataset 2005.

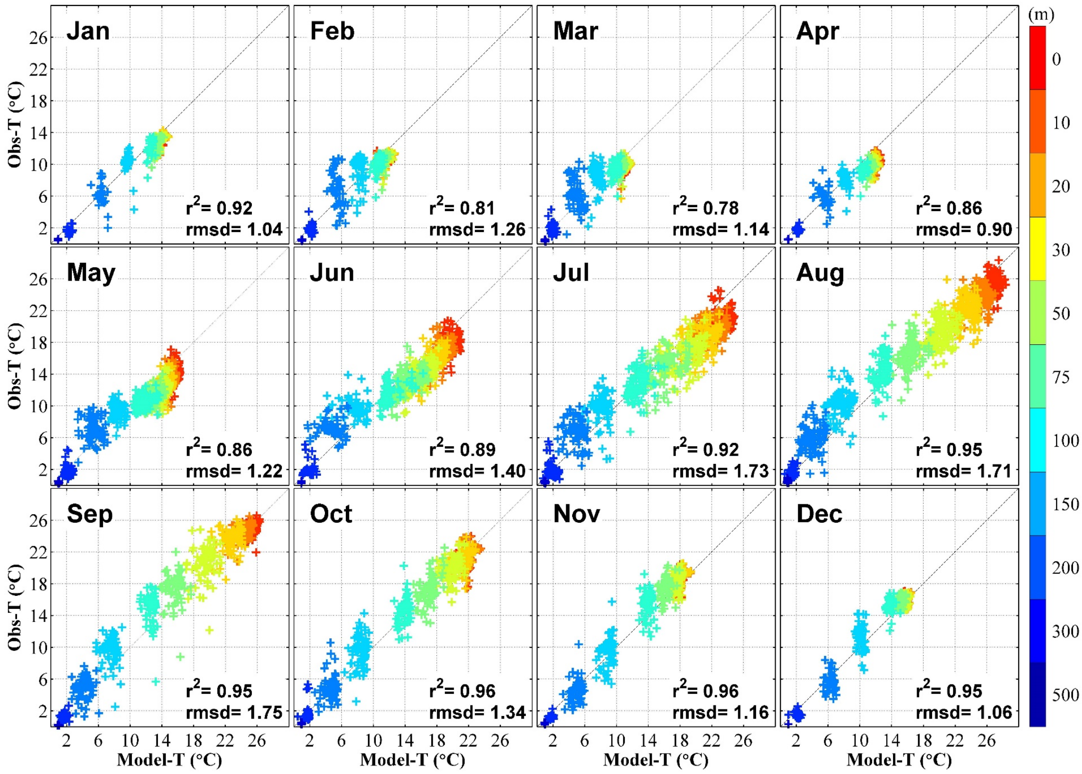
Jan
r2= 0.92
rmsd= 1.04
Feb
r2= 0.81
rmsd= 1.26
Mar
r2= 0.78
rmsd= 1.14
Apr
r2= 0.86
rmsd= 0.90
May
r2= 0.86
rmsd= 1.22
Jun
r2= 0.89
rmsd= 1.40
Jul
r2= 0.92
rmsd= 1.73
Aug
r2= 0.95
rmsd= 1.71
Sep
r2= 0.95
rmsd= 1.75
Oct
r2= 0.96
rmsd= 1.34
Nov
r2= 0.96
rmsd= 1.16
Dec
r2= 0.95
rmsd= 1.06
Obs-T (°C)
Model-T (°C)
(m)
0
10
20
30
50
75
100
150
200
300
500

(a)

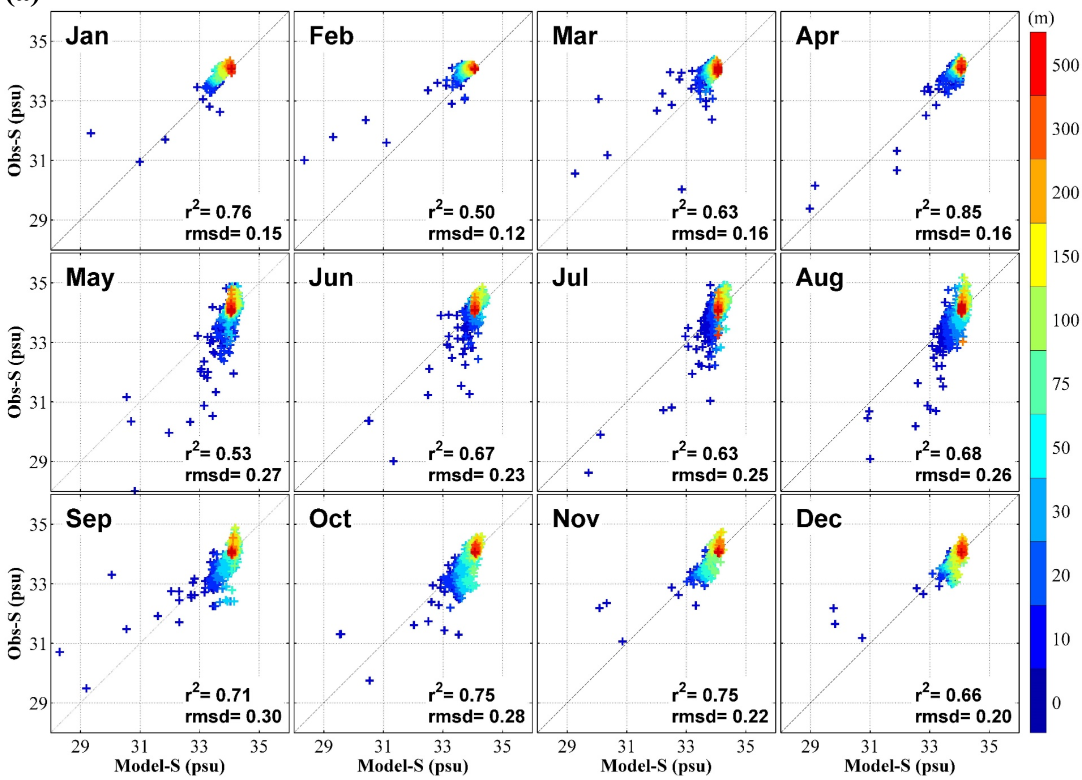
Jan
r2= 0.76
rmsd= 0.15
Feb
r2= 0.50
rmsd= 0.12
Mar
r2= 0.63
rmsd= 0.16
Apr
r2= 0.85
rmsd= 0.16
May
r2= 0.53
rmsd= 0.27
Jun
r2= 0.67
rmsd= 0.23
Jul
r2= 0.63
rmsd= 0.25
Aug
r2= 0.68
rmsd= 0.26
Sep
r2= 0.71
rmsd= 0.30
Oct
r2= 0.75
rmsd= 0.28
Nov
r2= 0.75
rmsd= 0.22
Dec
r2= 0.66
rmsd= 0.20
Obs-S (psu)
Model-S (psu)
(m)
500
300
200
150
100
75
50
30
20
10
0

(b)

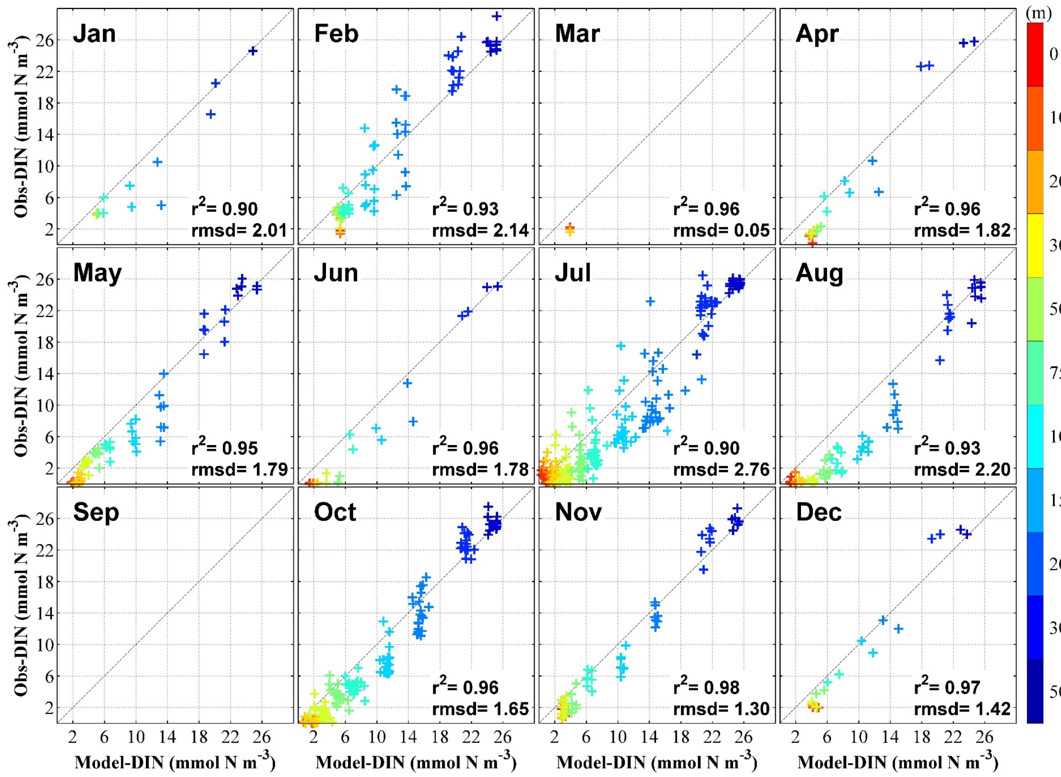

Jan
Feb
Mar
Apr
May
Jun
Jul
Aug
Sep
Oct
Nov
Dec
Obs-DIN (mmol N m-3)
Model-DIN (mmol N m-3)
r2= 0.90
rmsd= 2.01
r2= 0.93
rmsd= 2.14
r2= 0.96
rmsd= 0.05
r2= 0.96
rmsd= 1.82
r2= 0.95
rmsd= 1.79
r2= 0.96
rmsd= 1.78
r2= 0.90
rmsd= 2.76
r2= 0.93
rmsd= 2.20
r2= 0.96
rmsd= 1.65
r2= 0.98
rmsd= 1.30
r2= 0.97
rmsd= 1.42
(m)
0
10
20
30
50
75
100
150
200
300
500

(c)

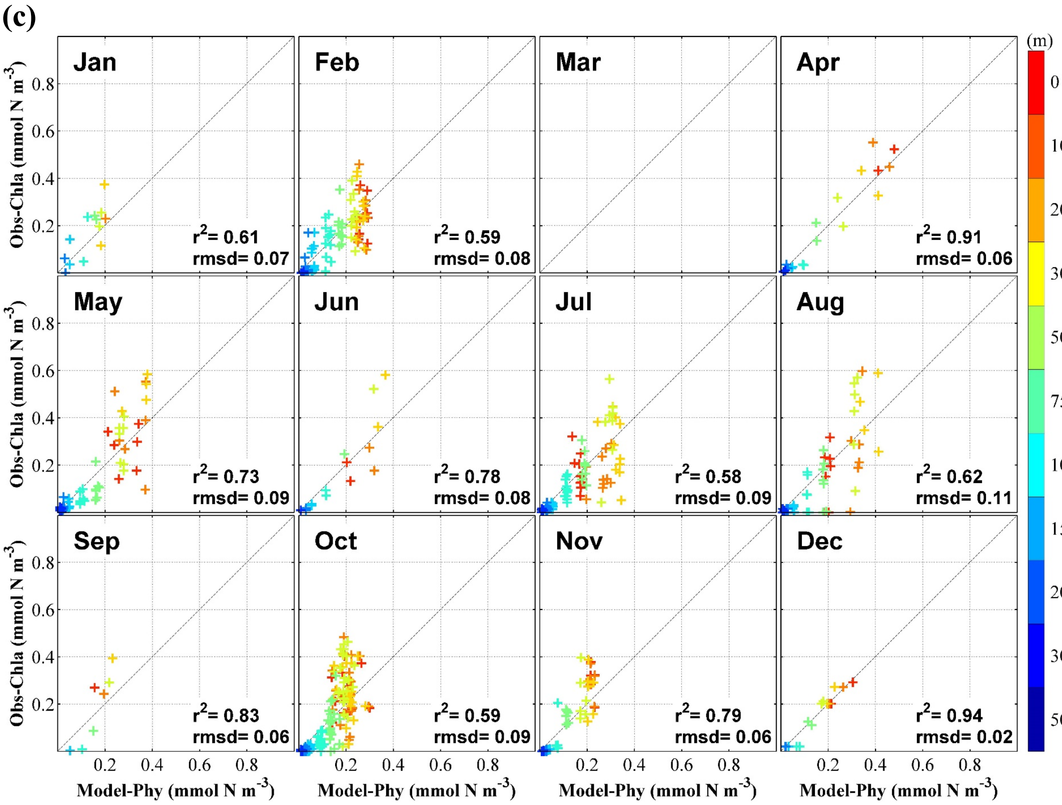

Jan
Feb
Mar
Apr
May
Jun
Jul
Aug
Sep
Oct
Nov
Dec
Obs-Chla (mmol N m-3)
Model-Phy (mmol N m-3)
r2= 0.61
rmsd= 0.07
r2= 0.59
rmsd= 0.08
r2= 0.91
rmsd= 0.06
r2= 0.73
rmsd= 0.09
r2= 0.78
rmsd= 0.08
r2= 0.58
rmsd= 0.09
r2= 0.62
rmsd= 0.11
r2= 0.83
rmsd= 0.06
r2= 0.59
rmsd= 0.09
r2= 0.79
rmsd= 0.06
r2= 0.94
rmsd= 0.02
(m)
0
10
20
30
50
75
100
150
200
300
500

(d)

Figure S3. Scatter plot of monthly data and model results for (a) Water temperature, (b) Salinity, (c) Dissolved inorganic nitrogen (DIN), and (d) Chl.a. The colors represent water depths.

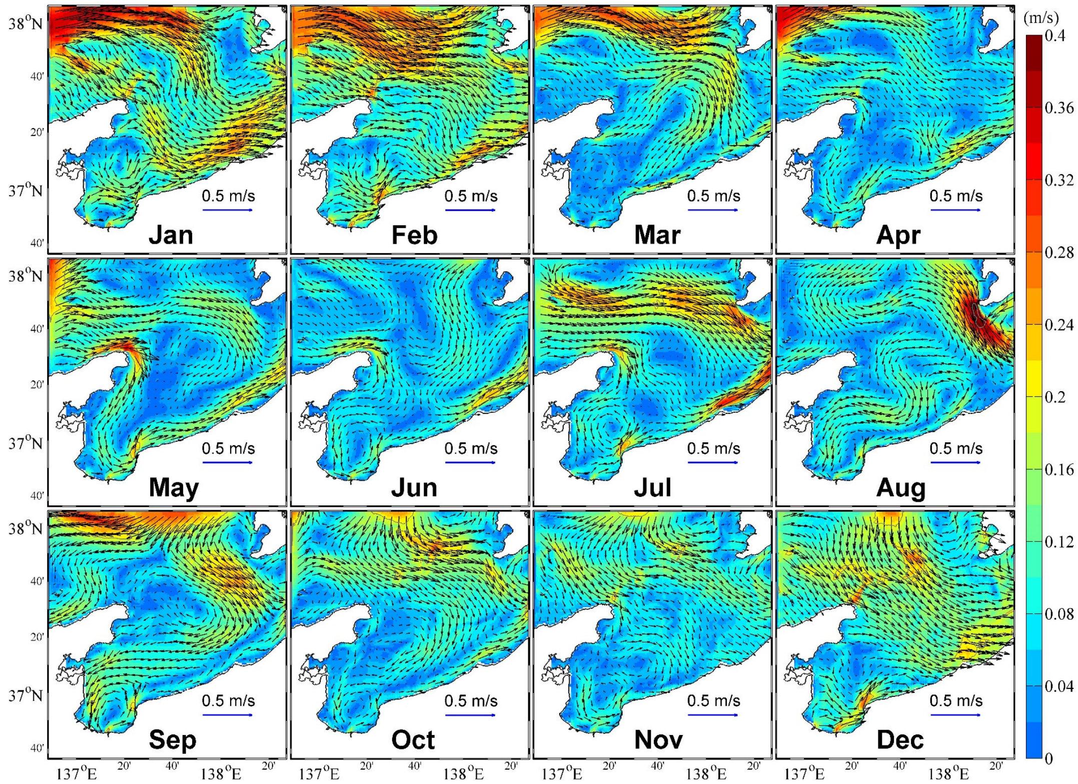

Figure S4. Monthly mean surface current. The black arrows represent the current direction and the colors represent the magnitude of the current.

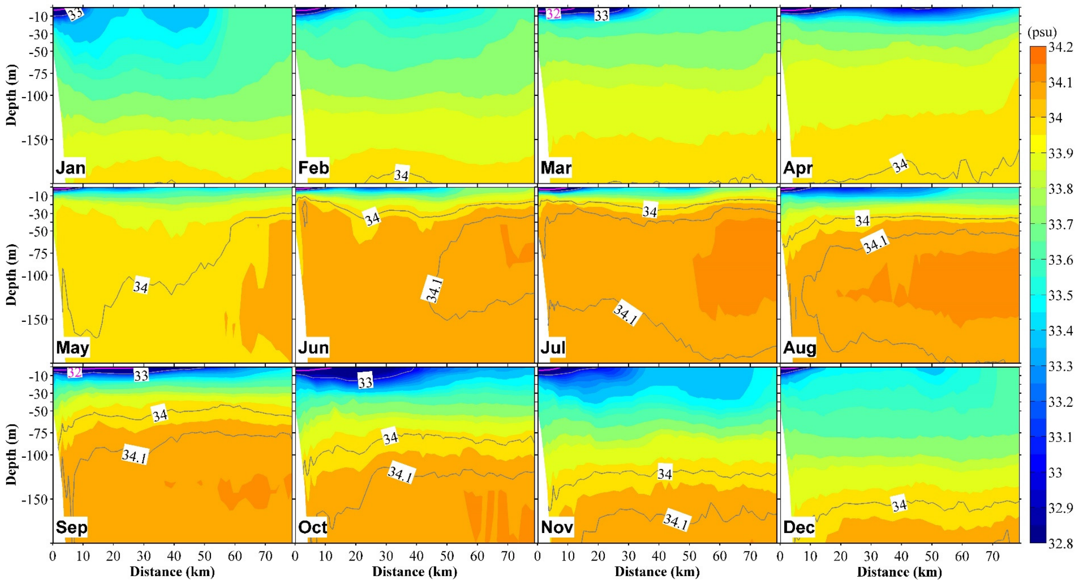

Figure S5. Vertical distribution at section S2 (in Figure 1b) of salinity in different months. The distance on the x-axis is measured from the shore.

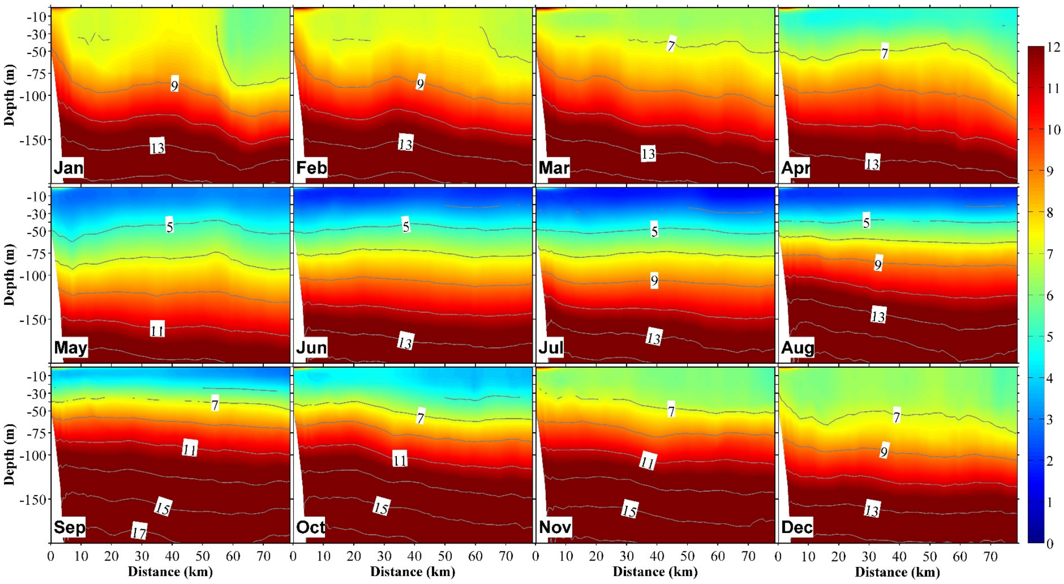

Figure S6. Vertical distribution at section S2 (in Figure 1b) of dissolved inorganic nitrogen (DIN) in different months, with the unit in mmolN m^{-3}. The distance on the x-axis is measured from the shore.

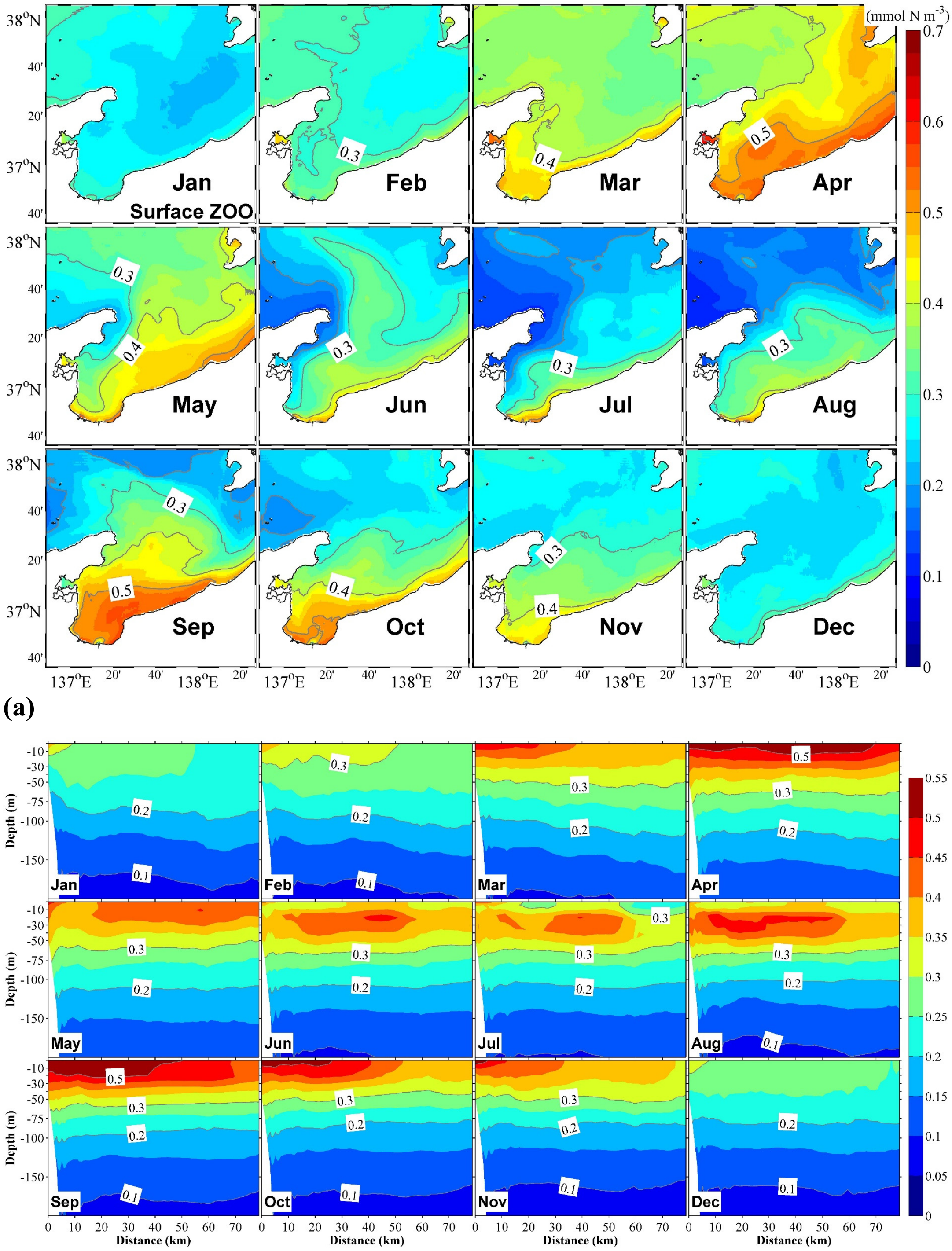

Figure S7. Distribution of zooplankton concentrations in different months. (a) Monthly mean surface zooplankton. (b) Vertical distritubion at section S2 (in Figure 1b) of zooplankton. The distance on the x-axis is measured from the shore.

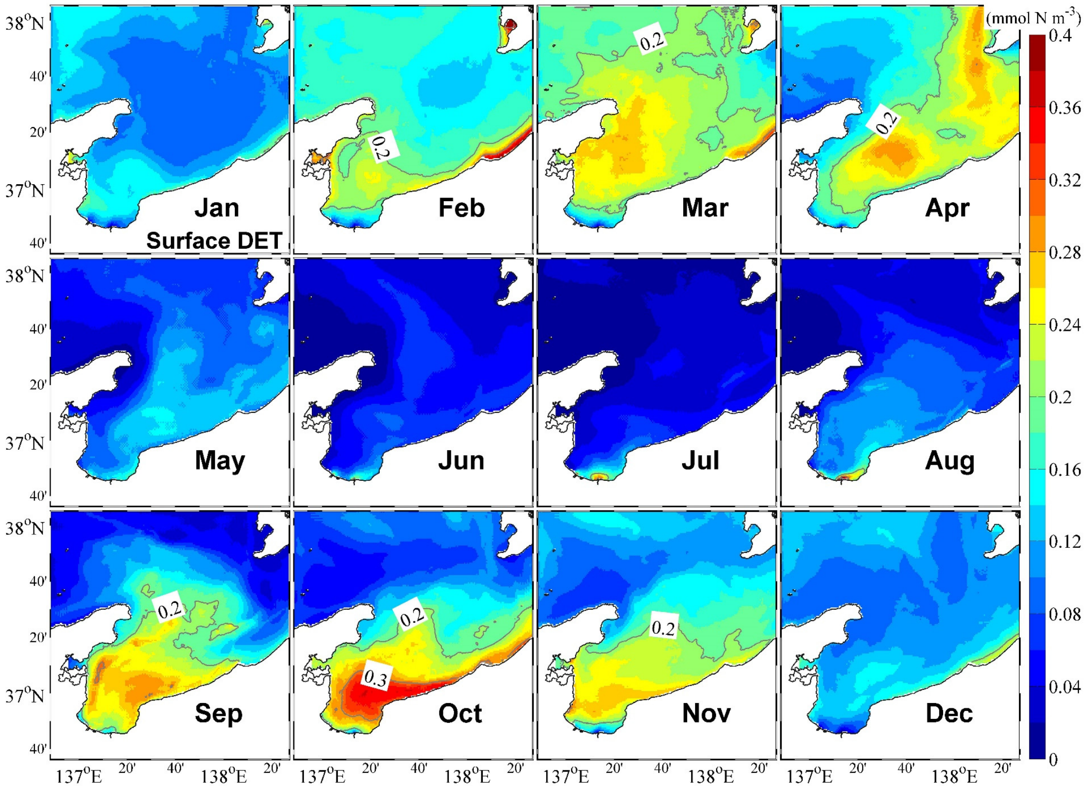

(a)

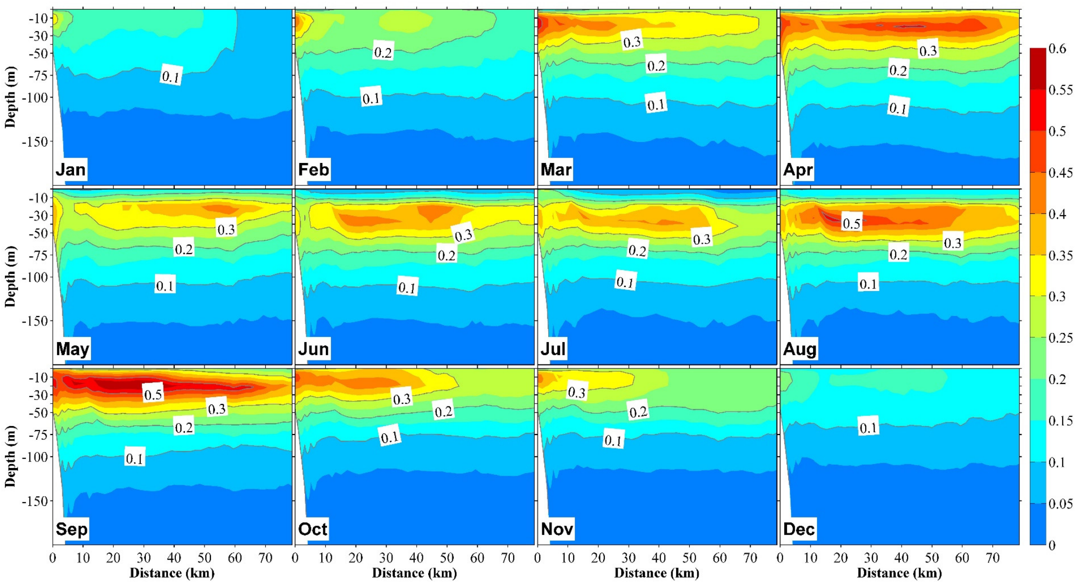

(b)

Figure S8. Distribution of detritus (DET) in different months. (a) Monthly mean surface DET, (b) Vertical distribution at section S2 (in Figure 1b) of DET. The distance on the x-axis is measured from the shore.

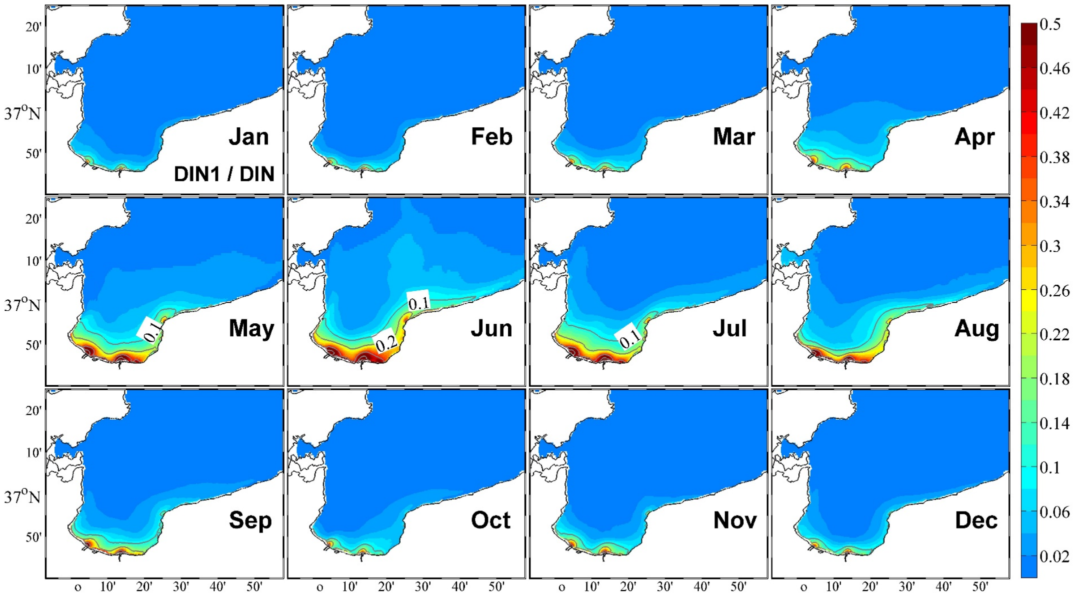

Figure S9. Contributions of dissolved inorganic nitrogen (DIN) originating from river water to total DIN in the surface layer (0–20 m) in different months.

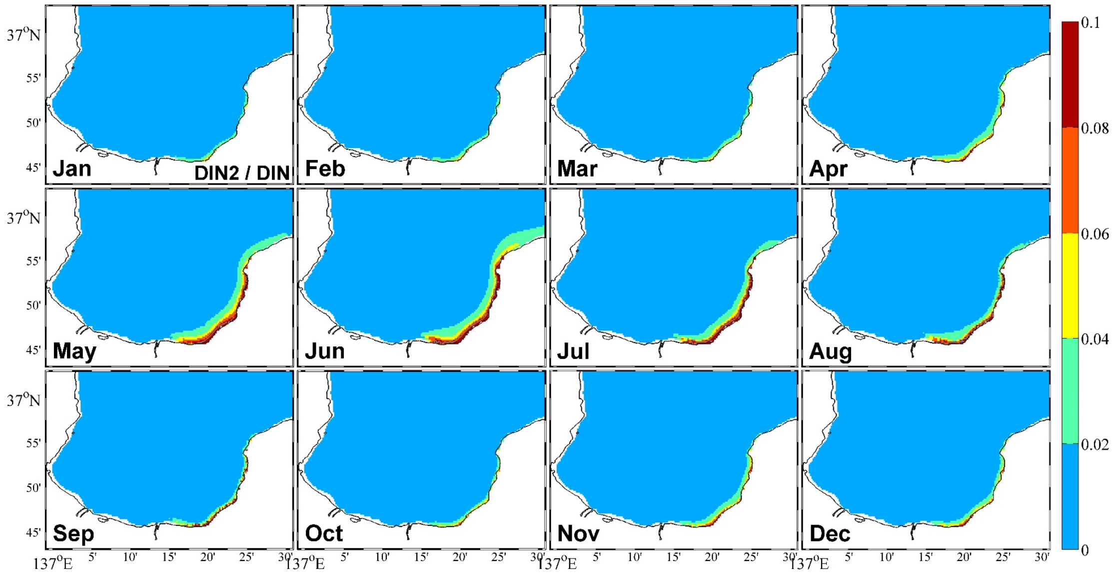

Figure S10. Contributions of dissolved inorganic nitrogen (DIN) originating from submarine groundwater discharge (SGD) to total DIN in the upper layer (0–70 m) in different months.

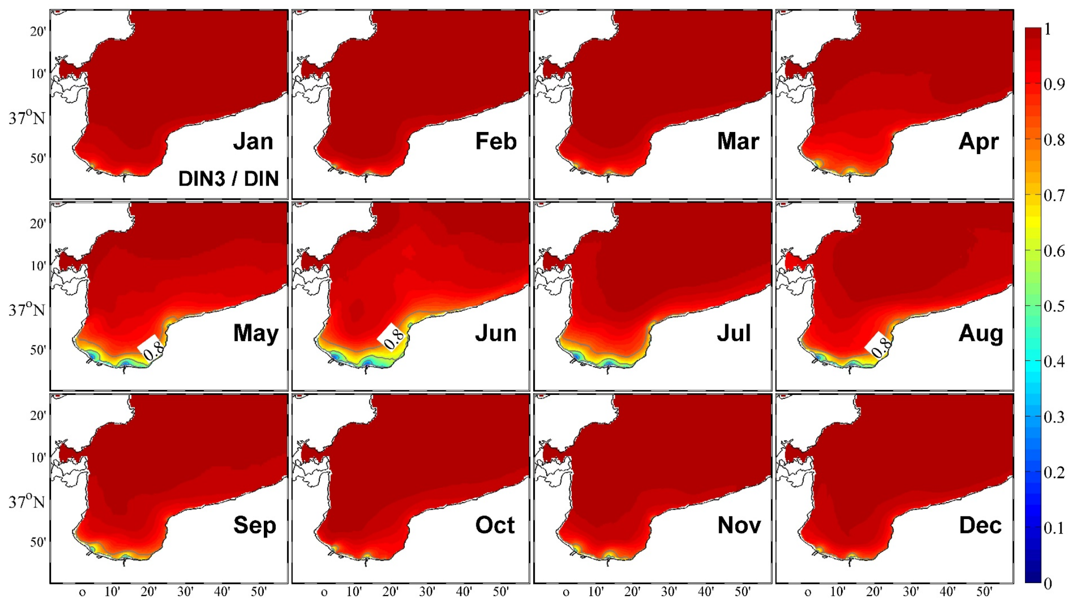

Figure S11. Contributions of dissolved inorganic nitrogen (DIN) originating from the Japan Sea to total DIN in the surface layer (0–20 m) in different months.

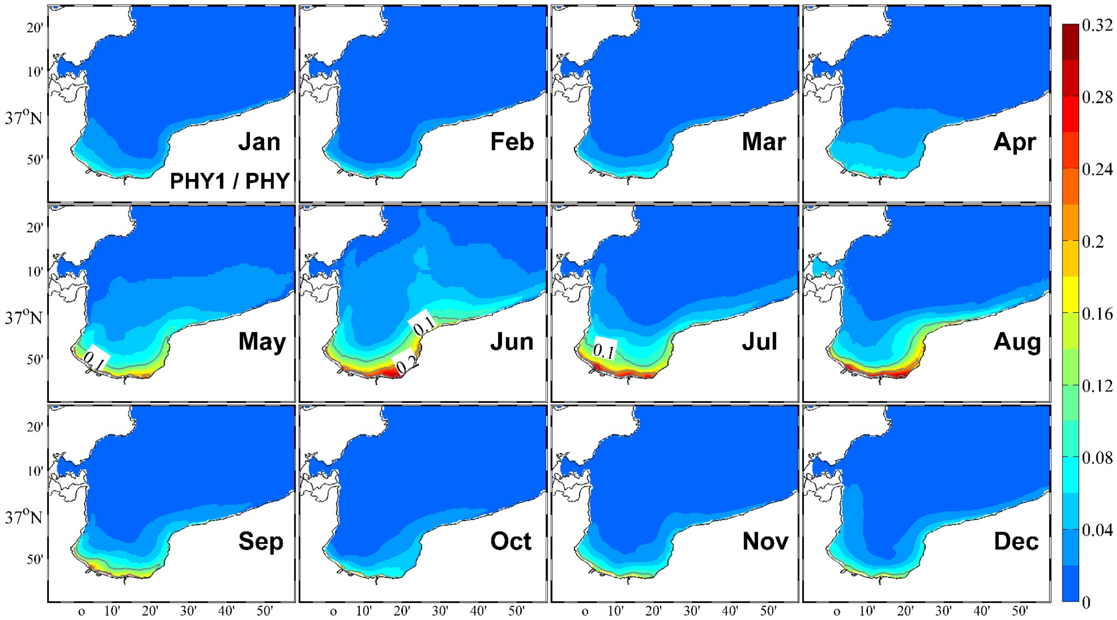

Figure S12. Distributions of the proportions of phytoplankton supported by nutrients originating from river water to the total phytoplankton in the surface layer (0–20 m) in different months.

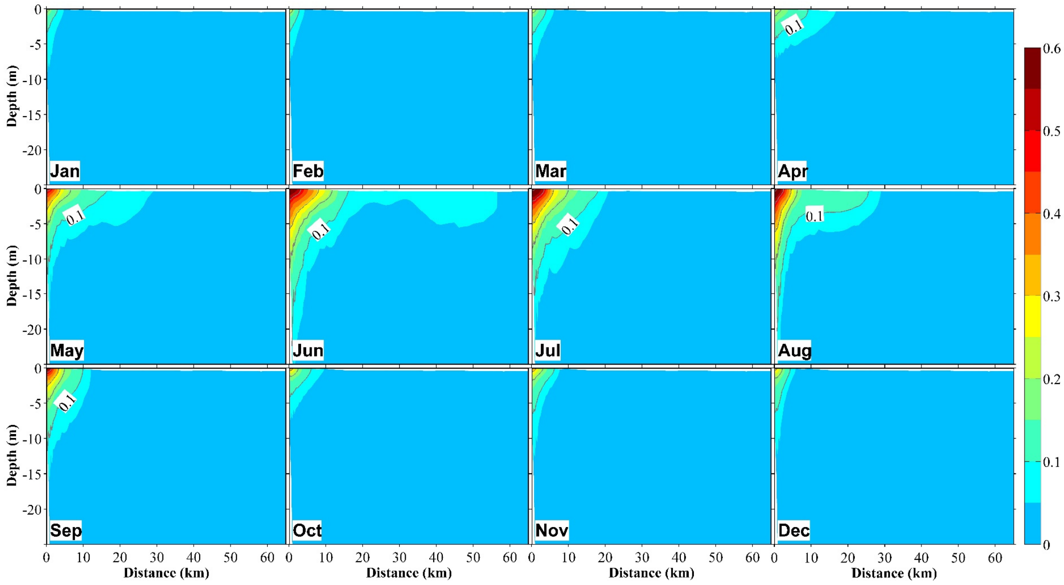

Figure S13. Vertical distribution at section S2 (in Figure 1b) of the proportions of phytoplankton supported by nutrients originating from river water to the total phytoplankton in different months. The distance on the x-axis is measured from the shore.

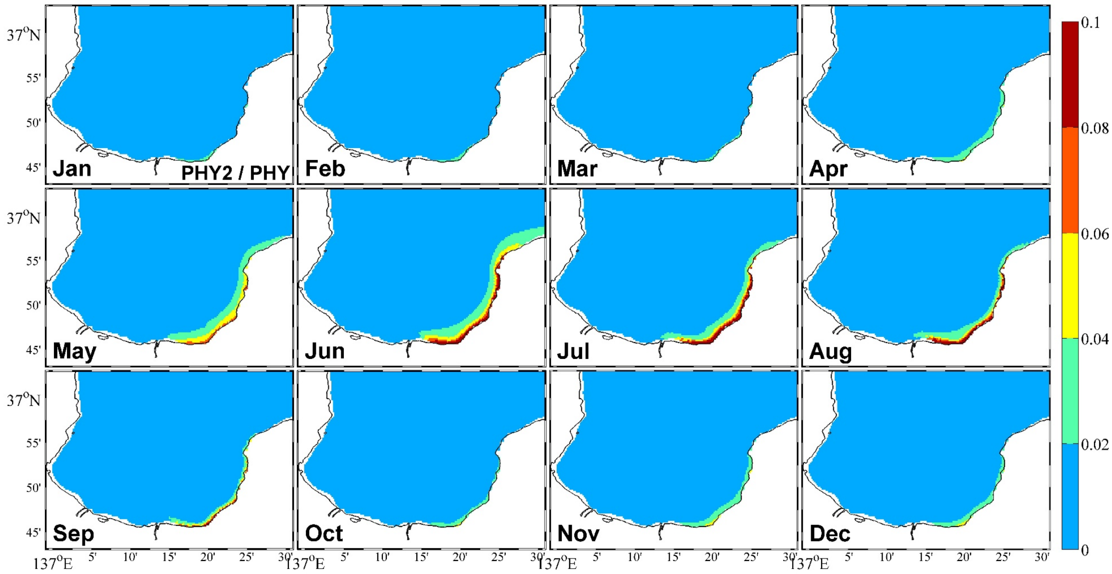

Figure S14. Distributions of the proportions of phytoplankton supported by nutrients originating from submarine groundwater discharge (SGD) to the total phytoplankton in the upper layer (0–70 m) in different months.

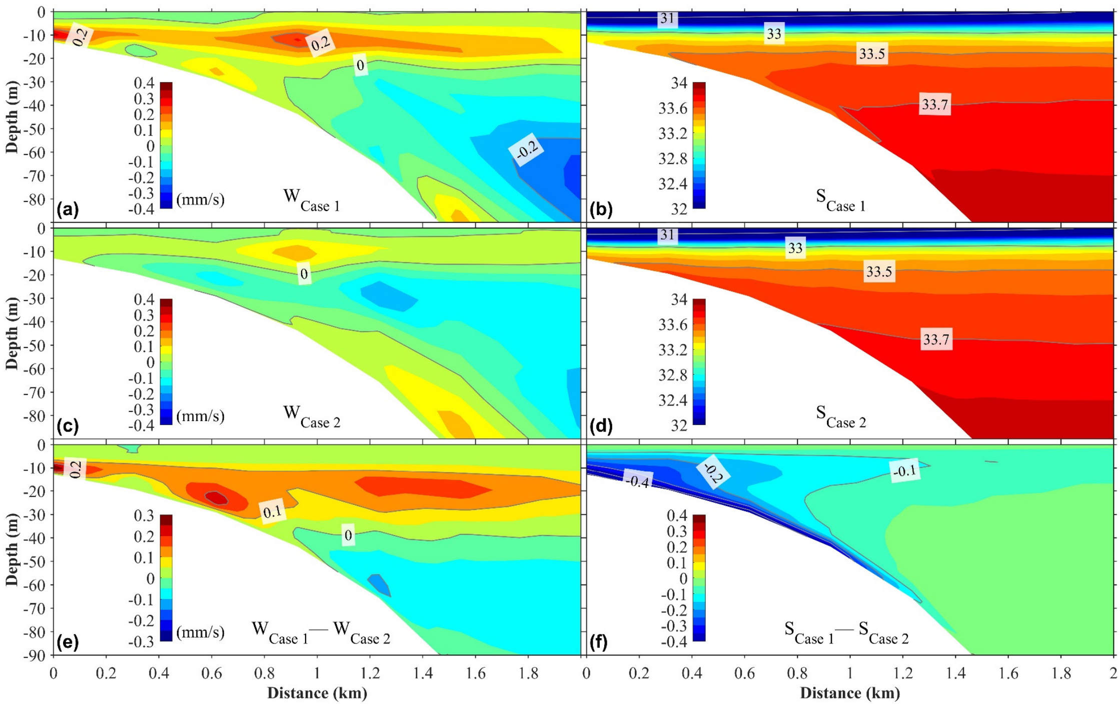

Figure S15. (a)−(d) illustrate the vertical distributions of the annual mean vertical velocity and salinity under two scenarios. Panels (a) and (b) correspond to Case 1, where the buoyancy effect of SGD is included in the hydrodynamic model, while panels (c) and (d) correspond to Case 2, where the buoyancy effect of SGD is excluded. (e) and (f) show the differences in vertical velocity and salinity between Case 1 and Case 2. The distance on the x-axis is measured from the shore.

References

Blumberg, A. F., & Mellor, G. L. (1987). A description of a three dimensional coastal ocean circulation model. In N. S. Heaps (Ed.), *Three-Dimensional Coastal Ocean Models* (Vol. 4). American Geophysical Union.

Eppley, R. W. (1972). Temperature and phytoplankton growth in the sea. *Fishery Bulletin*, *70*(4), 1063–1085.

Mellor, G. L. (1998). *USERS GUIDE for OCEAN MODEL. Program in Atmospheric and Oceanic Science*.

Onitsuka, G., & Yanagi, T. (2005). Differences in ecosystem dynamics between the Northern and Southern parts of the Japan Sea: Analyses with two ecosystem models. *Journal of Oceanography*, *61*, 415–433. https://doi.org/10.1007/s10872-005-0051-1

Sarmiento, J. L., & Gruber, N. (2006). *Ocean Biogeochemical Dynamics*. Princeton: Princeton University Press. Retrieved from https://doi.org/10.2307/j.ctt3fgxqx